Fluvial architecture as a response to two-layer lithospheric subsidence during the Permian and Triassic in the Iberian Basin, eastern Spain

José López-Gómez [a,*], Alfredo Arche [a], Henar Vargas [b], Mariano Marzo [c]

[a] Instituto de Geología Económica, CSIC-UCM, Facultad de Geología, Universidad Complutense, Antonio Novais 2, 28040 Madrid, Spain
[b] Repsol YPF. Paseo de la Castellana 280, 28046 Madrid, Spain
[c] Departament d'Estratigrafia, Paleontologia i Geociències Marines, Facultat de Geología, Universitat de Barcelona, Zona Universitaria de Pedralbes, 08071 Barcelona, Spain

ARTICLE INFO

Article history:
Received 3 November 2008
Received in revised form 16 November 2009
Accepted 27 November 2009

Keywords:
Fluvial architecture
Subsidence
Stretching factor
Permian
Triassic
Tectonic controls

ABSTRACT

The stratigraphy of a sedimentary basin is mainly the result of the long-term response of a depositional surface to prolonged subsidence. However, the real nature of interrelations between fluvial architecture and subsidence is still unknown. Herein, we present new data on these relationships by combining the results of detailed sedimentological field work with data acquired through automated forward modelling and backstripping for the alluvial Permian and Triassic sediments of the SE Iberian Ranges. Using this methodology, we determined tectonic subsidence of the basin by means of backstripping analysis and crust and lithospheric mantle stretching factors (δ and β, respectively) using forward modelling technique. Results indicated that a configuration of two individual and independent layers during lithospheric subsidence for each tectonic phase fit better for this time of the studied basin evolution than the assumption of subsidence due to a single layer spanning the whole lithosphere.

For this study, we simplified fluvial geometries as two main types: isolated (I) and amalgamated (A), with subtypes in each case. Different order bounding surfaces (b.s.) were distinguished in the field, although we only selected those affecting the whole basin under study. These included those b.s. of clear tectonic origin, ranging from individual basin boundary-fault pulses produced over periods of approximately 1 My to those arising from major tectonic events, such as the beginning of extension in the basin, causing major changes in basin geometry over periods of 3–5 My.

The comparison of δ and β values and fluvial geometries for each identified tectonic phase in the basin evolution, revealed some possible relationship between subsidence and fluvial geometry: Sections showing the most varied fluvial architectural geometries, including ribbon and nested forms, were related to higher β and δ stretching factors values indicating tectonic phases of greater stretching and subsidence. When both stretching factors were similar and close to 1, fluvial geometry was basically reduced to amalgamated geometry type. Wider ranging of fluvial geometries was associated with stages of basin development in which crust and upper mantle activities differed, that is, showing larger differences of β and δ stretching factors values. The related slope changes are proposed as the main surface control of fluvial styles.

Combination of subsidence with other possible controlling factors such as avulsion rate, climate or budget of sediments, gives rise to the definitive alluvial architecture of a basin.

1. Introduction

Sedimentary basins form by deformation of the lithosphere, and their stratigraphical record is the sum of a number of geological processes, mainly allogenic (basically climate and tectonics), which interact with each other through time and may cause relative sea-level changes. Thus, a long-term response of the depositional surface to prolonged subsidence will determine the stratigraphy of a sedimentary basin.

Stratigraphical modelling techniques developed over the last three decades have provided geologists with a powerful tool for examining and comparing the different processes that lead to the sedimentary record of a particular basin. The basic assumption of basin analysis techniques is that similar genetic processes show a consistent vertical pattern in their sedimentary evolution.

Studies since the seventies on lithosphere deformation by stretching and rapid cooling have been conducted in practical synchrony with those evaluating intracontinental rifts and passive margins. Rifts were soon related to thermal anomalies existing at depth. Convection appears to be sufficiently rapid to explain rift uplifts when the basal heat flow from the asthenosphere is several times higher than the normal rate (Allen and Allen, 1990). However,

* Corresponding author.
E-mail address: jlopez@geo.ucm.es (J. López-Gómez).

recent results also suggest there is no need in some cases to invoke hypothetical plume activity to explain the mechanism destabilizing the lower lithosphere, and that passive-driven intraplate extension provides an efficient alternative (Huismans et al., 2001).

Whichever the case, lithosphere deformation is a prerequisite for basin formation and subsequent refilling. Deformations caused by stretching of the lithosphere are normally explained by assuming the crust and lithospheric mantle extend by similar amounts (uniform stretching) (McKenzie, 1978) or by non-uniform amounts (Salveson, 1976, 1978; Royden and Keen, 1980), whereby stretching is then depth-dependent. The latter mechanism is based on a different rheological response of the crust and lithospheric mantle to stretching, and thus a different stretching factor is proposed for each one (δ and β respectively). In contrast, the uniform stretching theory only requires one factor (β) for calculations referring to a uniform lithosphere. A more complete idea of the stretching changes produced in a basin was developed by Steckler (1981), who suggested several short extensional phases followed by cooling in the general extension process. It is important to stress that the amount of subsidence is not the unique factor controlling fluvial styles, as sediment supply, hydraulic regime and climate also must be considered. However, subsidence rate is the main control on the general configuration of extensional sedimentary basins and a major factor creating surperficial topographic gradients and, consequently, fluvial styles in the sedimentary record.

Basins of similar genetic type may show a consistent pattern in their sedimentary development. Accordingly, a formative mechanism of a basin such as subsidence has predictive power in assessing basin-fill (Allen and Allen, 1990). Works relating subsidence changes in rift basins to their refill style involve detailed field work based on well-exposed outcrops, such as those described by Alexander and Leeder (1987), Leeder (1993) and Steel and Ryseth (1990), among others. Several related models have been proposed to explain the architectural arrangement of channel stacking patterns in alluvial sequences. Some of these models (e.g., Allen, 1978; Bridge and Leeder, 1979) have been widely used to quantify relationships between subsidence and large-scale fluvial architecture in sedimentary basins, although none of them can be taken as definitive. One of the reasons for this is that we have no precise models to quantify results when various autocyclic processes act at the same time in different ways. Furthermore, results from experiments conducted in laboratories are commonly inconsistent and also conflict with the results obtained by introducing data from processes such as avulsion in the analysis (see e.g., Heller and Paola, 1996; Ashworth et al., 2004). As will be discussed later on, it seems that the interrelation between subsidence and large-scale fluvial architecture should be approached with caution, because there is no direct link between this tectonic process and the 3-D configuration of the sediments. As mentioned above, topographic gradient and its changes are the primary controlling factor (largely, but not exclusively, of tectonic origin).

For the Permian–Triassic eastern Iberian intracratonic basin, E Spain (Fig. 1A), van Wees et al. (1998) related temporal and spatial variations in tectonic subsidence to stratigraphy, based on both high-resolution backstripping analysis and automated forward modelling. This type of analysis is marked by a large number of rifting pulses, many more than documented in previous studies (Sánchez-Moya et al., 1992; Salas and Casas, 1993; Arche and López-Gómez, 1996) since the rift phases are of low magnitude, very short-lived and can be remarkably well correlated over the whole basin. Each defined phase has its own stretching factor (β, for the lithosphere mantle and δ for the crust) data and this increased resolution in subsidence data leads to better resolution of the tectonic signal allowing the efficient and very accurate assessment of temporal and spatial relations in lithospheric rift dynamics. Recently, Vargas et al. (2009) also used this technique to describe a two-layer lithospheric subsidence model for the same basin focussing on the Permian and Triassic periods. In the present report, by means of backstripping analysis of subsidence, the automated forward modelling technique and a detailed sedimentological study of Permian and Triassic alluvial sediments of the area cited above, we analyse and discuss the possible relationship between the presence or absence of different large-scale fluvial architecture types and the stretching factors (β and δ) calculated for each differentiated subsidence phase. As far as we are aware, this is the first time this combined theoretical/practical approach has been used to correlate fluvial architecture with subsidence in this area.

2. Geological setting

The present-day Iberian Ranges constitute part of an intracontinental fold chain in the northeast of the Iberian microplate, which formed after Palaeogene tectonic inversion of the Mesozoic Iberian intracratonic basin (Guimerá and Álvaro, 1990; Arche and López-Gómez, 1996). The range is an intraplate chain bounded by the Central System and the Tagus Basin to the west, the Catalonian Ranges to the northeast, and the Cenozoic Ebro Basin to the north (Fig. 1). Its present configuration shows two Palaeozoic–Mesozoic branches, the Castilian and the Aragonese (south and north, respectively) separated by the Cenozoic Teruel Basin.

Three main normal-lystric NW–SE trending basin boundary faults define what was the Iberian Basin during Permian and Triassic times: the Majadas–Gátova or Serranía de Cuenca, the Molina de Aragón–Teruel–Chóvar and the Montalbán–Castellón (Arche and López-Gómez, 1996) (Fig. 1). These fault systems are related to ancient Hercynian or older structures that controlled the location of the Early Permian basins which were later to evolve during the Cenozoic after tectonic inversion to thrust faults. A subordinate but not less important palaeogeographical NE–SW trending fault system was also active in the Iberian Basin since the Early Permian, but this system did not become essentially active until the Anisian (Middle Triassic).

From the large differentiated number of rifting pulses three main rifting phases of deposition have been selected and described for Permian–Middle Triassic times in the Iberian Ranges (van Wees et al., 1998). A first, local phase of Autunian (Early Permian) age that formed isolated small basins, a second, Late Permian phase affecting almost all the Iberian Ranges, which was clearly conditioned by a NW–SE trending ancient lineament structure (López-Gómez and Arche, 1993a), and a third phase involving a long period of thermal subsidence during the Early–Middle Triassic. A punctual phase, and so not studied here, was detected in the Molina de Aragón–Majadas area during the Late Permian–Early Triassic. Vargas et al. (2009) recently demonstrated that these three phases can be recognized in other Permian–Triassic basins of the Iberian Plate, although starting and finishing times do not always coincide.

3. The sediments

There have been numerous descriptions since the seventies of the Permian–Triassic sediments of the eastern Iberian Ranges (Pérez-Arlucea and Sopeña, 1985; Sopeña et al., 1988; López-Gómez and Arche, 1993a,b, 1997; Arche and López-Gómez, 1999a,b; López-Gómez et al., 2002). Permian and Lower Triassic sediments appear as a succession of well-exposed alluvial units, while the Middle (Röt and Muschelkalk facies) and Upper Triassic are represented by mixed and shallow marine deposits (Fig. 2).

Alluvial sediments occur as five units from bottom to top: Tabarreña Breccias, Boniches Conglomerates, Alcotas Siltstones and Sandstones, Cañizar Sandstones and Eslida Siltstones and Sandstones. All of them have been formally described as formations (López-Gómez et al., 2002). The ages of all of these formations have been inferred from their pollen and spore associations (Boulouard and Viallard, 1982; Doubinger et al., 1990; Sopeña et al., 1995) except for the Tabarreña Fm. Two depositional sequences (A and B) have been

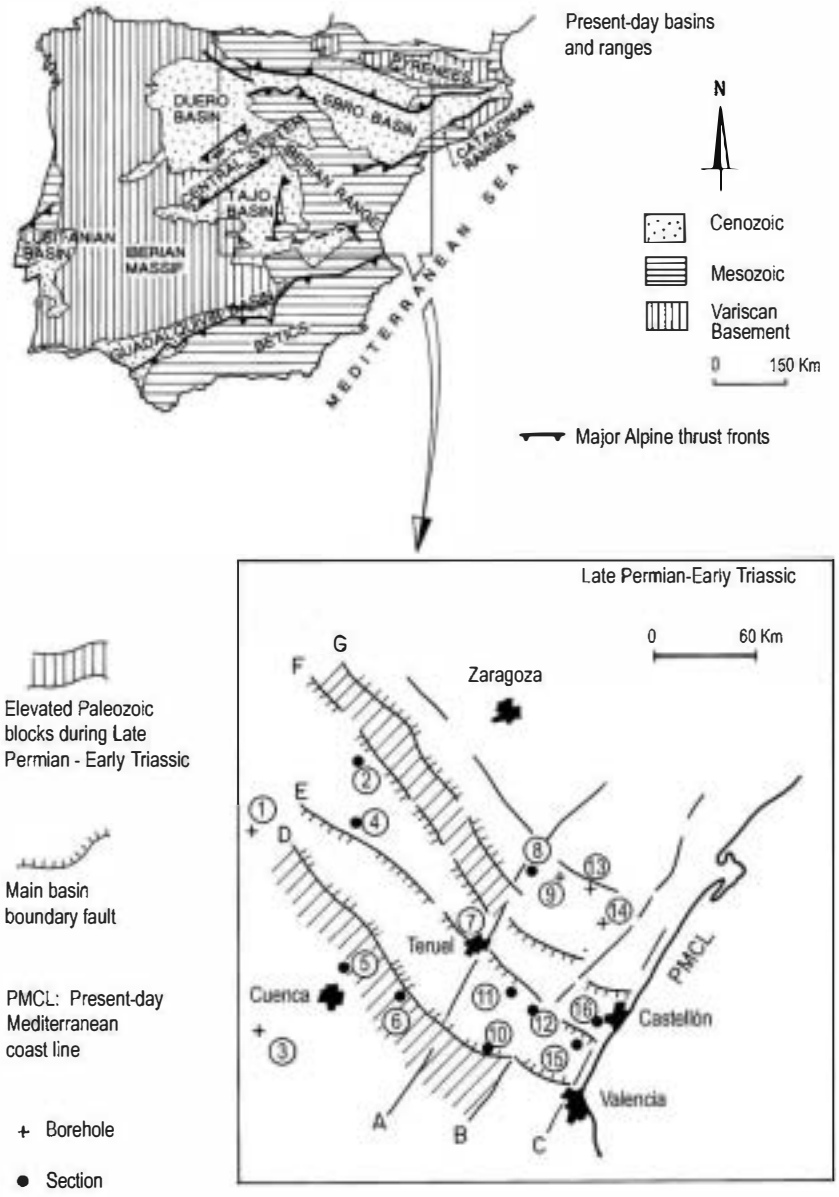

Fig. 1. Above: Present-day basins and Ranges in the Iberian Peninsula. The Iberian Range shows two branches (north or Aragonese and south or Castilian) separated by the Tertiary Teruel Basin. Below: Location of the studied sections and boreholes and Late Permian–Early Triassic fault lineaments basin boundary faults and elevated Paleozoic blocks. 1 — Torralba, 2 — Alhama, 3— ElHito, 4 — Molinade Aragón, 5 —Majadas, 6 — Cañete, 7 — Teruel, 8 —Montalban, 9 —Miranbel, 10— Chelva, 11 —Manzanera, 12 — Jérica, 13 —Bobalar, 14 — Salsadella, 15 —Gátova, and 16 — Chovar–Eslida. Main tectonic lineaments: A — Teruel, B — Requena, C— Valencia–Castellón, D — Cañete–Sagunto, E— Molina–Teruel, F —Alhama–Oropesa, and G —Ateca–Montalbán.

discerned through a detailed stratigraphical study. Depositional sequence A is constituted by the Boniches and Alcotas Fms and depositional sequence B comprises the Cañizar and Eslida Fms. All of these units are irregularly deposited across the Iberian Basin, and are clearly conditioned by a significant basal palaeorelief and subsequent synsedimentary tectonic influence as will be discussed later on. Their main stratigraphical features are:

The Tabarreña unit. This unit never exceeds a thickness of 30 m and contains scree deposits with very angular quartzite clasts up to 45 cm in size. Clasts may be matrix- or clast-supported. Although there are no palaeontological data, the unit is considered Autunian (Lower Permian) by correlation with proximal areas (López-Gómez and Arche, 1993a). This formation shows a very reduced cropping area (less than 1 km^2) and clearly belongs to a previous tectonic cycle, such that it is outside the scope of this work.

The Boniches Fm. Comprised of 3–4 m thick packets of conglomerates bounded by erosive surfaces or centimetre-scale sandstone levels (Fig. 3A), this unit only developed in the area Cañete to Chelva. Overall thickness is less than 88 m. Its conglomerates consist of subangular to well-rounded quartzite pebbles (up to 40 cm) organized in upward-fining composite sequences about 1.2 m thick. Sandstones are comprised of quartz, phyllosilicates, haematite and feldspars, while XRD analysis of isolated fine sediment levels reveals illite, kaolinite and pyrophyllite. Palaeocurrent trends indicate a NE direction in the lower part of this unit and towards the SE in the middle and upper parts. Its age is Thüringian (Upper Permian). A more detailed description of this formation can be found in López-Gómez and Arche (1997).

The Alcotas Fm consists of red siltstones and clays, associated lenticular sandstone bodies and sporadic conglomerate bodies

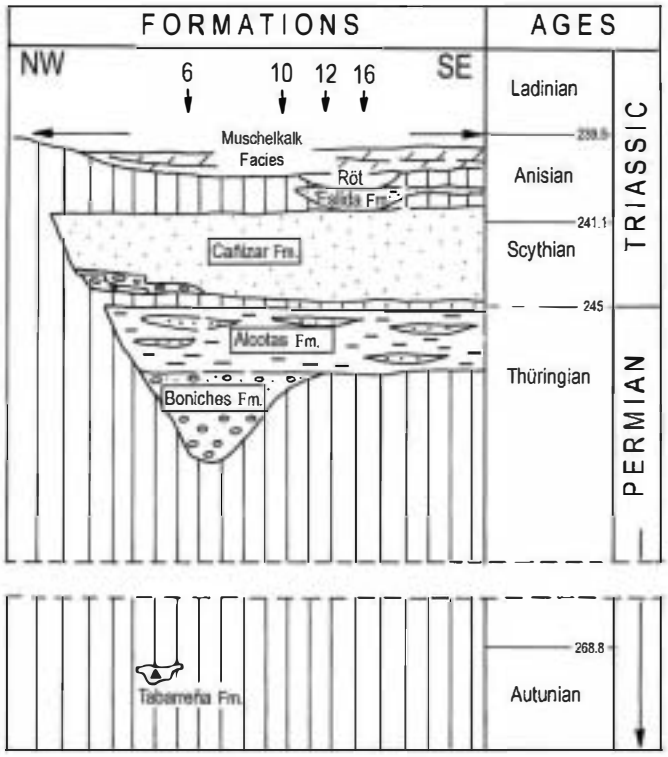

Fig. 2. Late Permian–Early Triassic stratigraphy of the studied area. Studied formations are: Boniches, Alcotas, Cañizar and Eslida. Locations: 6 — Cañete, 10 — Chelva, 12 — Jérica, and 16 — Chovar–Eslida. See Fig. 1 for their locations. Ages from Gradstein et al. (1995).

(Fig. 3B). This formation appears throughout the study area and can attain a thickness of 170 m. Sandstones are mainly arkoses and the clay fraction mainly consists of illite and quartz. Sandstone and conglomerate bodies constitute upward-thinning and -fining sequences generally less than 1 m thick. When well-developed, these bodies show an erosive base and never exceed a few hundred meters in width, whilst small bodies have a planar base and never surpass a hundred meters. Palaeocurrents consistently trend towards the SW. Its age is Thüringian (Upper Permian). This formation is described in detail in López-Gómez and Arche (1993a).

The Cañizar Fm. This formation, comprised of red pink sandstones, appears across the whole study area and can reach 170 m in thickness. Sandstones are compositionally arkoses, illite and quartz cemented with K-feldspar. Palaeocurrent trend analyses consistently indicate SE. Sandstone bodies consist of upward-thinning and -fining sequences, tens of centimetres thick that constitute up to six packets of some 20 m in thickness separated by major boundary surfaces (Fig. 3C). The top of the formation is dated Anisian (Middle Triassic) but the base is less well constrained and could be Scythian (Induan or Olenekian, Lower Triassic). This would indicate a long period of slow, intermittent deposition. This formation is described in detail in López-Gómez and Arche (1993b).

The Eslida Fm. Comprising red siltstones and intercalated decimetre-scale sandstone bodies of arkosic composition, this formation only crops out in a narrow area of the SE Iberian Ranges but can attain a thickness of 660 m. Intercalated sandstone bodies show different

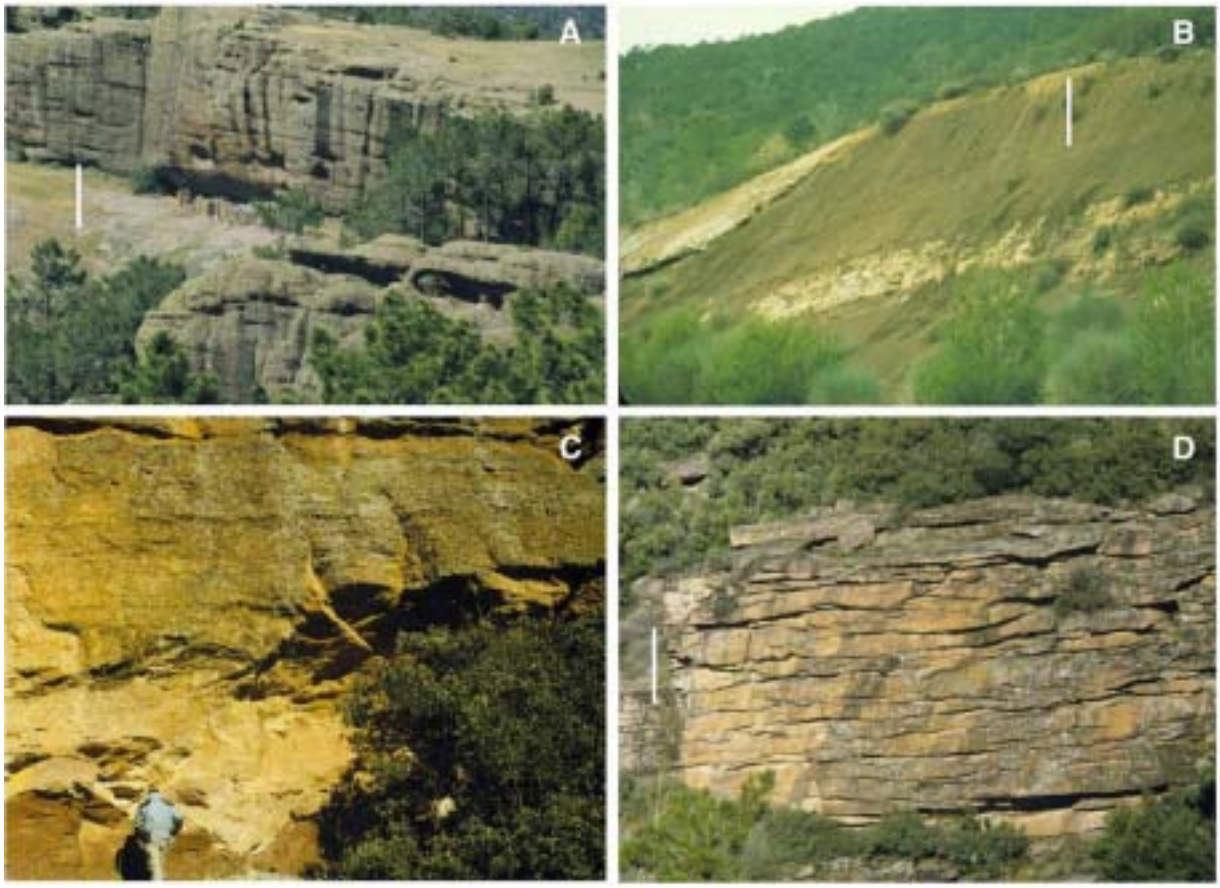

Fig. 3. Field photographs of the studied formations: A — Boniches Fm., B — Alcotas Fm., C — Cañizar Fm., and D — Eslida Fm.

sedimentary architectural types, normally formed by successions of elementary thinning- and fining-upward sequences less than 80 cm thick (Fig. 3D). The palaeocurrent trend is disperse indicating a S and SE direction. The Eslida Fm is the youngest alluvial unit preceding the transgression of the Tethys in the Iberian Peninsula. This formation is Anisian (Middle Triassic) in age and is described in detail in Arche and López-Gómez (1999a).

4. Alluvial style and architecture of sediments

Our evaluation of the sediments was performed on fifteen complete and twenty one incomplete sections all in good-quality outcrops (Fig. 1). Given that detailed sedimentological studies of all the units described have been published previously (López-Gómez and Arche, 1993b, 1994, 1997; Arche and López-Gómez, 1999a,b), in this chapter we will only present data considered necessary.

4.1. Alluvial style

The alluvial style of the units is defined by two main characteristics: lithofacies and channel morphologies, as well as the refill of channels and their relationship with floodplains. These characteristics constitute what is called the body type (conglomerate or sand-body geometries), represented here as channels, bedforms and sheets. The nomenclature used for these body types was according to Friend (1983), Hirst (1991) and Miall (1985, 1996) as well as our own terms defined here. Lithofacies codes were taken from Miall (1996). Table 1 summarises the alluvial styles observed in the units through definition of the main body types mentioned above for each one and their main characteristics. The main findings of these analyses indicate the following:

The Boniches and Cañizar Fms show a generally constant style whilst the Alcotas and Eslida Fms have different internal styles according to locations. Except for the lower part, probably related to proximal alluvial fans, the Boniches Fm was deposited in a shallow gravel braided fluvial system deposited by perpendicular paleocurrents to those of the basal, isolated alluvial fans (López-Gómez and Arche, 1997). Similar examples are described in Middleton and Trujillo (1984) and Ramos and Sopeña (1983).

The Alcotas Fm shows sandy low-sinuosity braided, sheetflood distal braided and isolated sandy meandering fluvial styles in floodplain deposits (Arche and López-Gómez, 1999b), similar to examples described by Rust and Legun (1983), Cotter and Graham (1991) and Alexander (1992). A general decrease in the energy of these fluvial systems can be clearly appreciated towards the top of the unit.

The Cañizar Fm presents a sandy stable (shallow and deep) braided fluvial style with dominant bedload transport (López-Gómez and Arche, 1993b). Similar examples have been described in detail by Cant and Walker (1978), Crowley (1983) and Haszeldine (1983).

The Eslida Fm is the most complex one, since it comprises the five different fluvial styles defined previously: sandy low sinuosity braided, sandy stable braided, sheetflood distal braided, anastamosed, and sandy meandering (Arche and López-Gómez, 1999a). The presence or absence of these fluvial styles in the sections depends on the onlap relationship type with the basement. Similar examples in ancient sediments have been also described by Cotter and Graham (1991), Rust and Legun (1983), Olsen (1988) and Nanson and Croke (1992).

4.2. Alluvial architecture

Alluvial architecture is the geometric response to the different alluvial styles in terms of the stacking of sediments. Hence, a body type is a channel, laminated sand sheet or sandy bedform with particular facies and characteristics or body type groups could give rise to characteristic fluvial architectural bodies (Miall, 1985; Eberth and Miall, 1991; Fielding, 1993; Miall, 1996) or body geometries.

Table 1
Summary of the main sedimentological characteristics and their interpretations of the alluvial deposits of the studied units in the SE Iberian Basin. Code of facies based on Miall's classification (1996). Differentiated body types are described in Fig. 4.

Body type: channels, bedforms and sheets	Lithology (after Miall, 1996)	Characteristics	Alluvial styles interpretation	Location (in the study area) and general references
Amalgamated complexes of gravel bedforms (A)	Gm, Gp, Gt	Amalgamation of massive or crudely bedded bodies. Fining-up sequence <1 m. Storeys: 2–5 m thick	Braided fluvial system with longitudinal and transverse bars. Channel fill. Presence of waning flows	Boniches Formation (Ore, 1964; Middleton and Trujillo, 1984; Nemec and Postma, 1993)
Amalgamated complexes of sand bedforms (A)	St, Sp, Sh, Sl, Sr, Se, Ss	Amalgamation of different channels and elementary and composite bedforms	Braided fluvial systems with transverse and linguoid bedforms. Channel fill	Eslida and Caflizar Formations (Bluck, 1976; Allen, 1983; Marzo and Anadón, 1987)
Sheet sandstone, multilateral/ multi-storey (j)	St, Sp, Sh, Sl, Sr, Se, Ss	Lenticular bedded with mainly longitudinal progradation. Width <600 m. Many storeys compose the sheets	Isolated lenticular bodies composed of transverse and linguoid bars and channels	Eslida and Alcotas Formations (Horne and Fern, 1976; Røe and Hermansen, 1993)
Semi-permanent isolated channels (I)	St, Sp, Sh, Sl, Se and less commonly Gp, Gt	Width <200 m, 2–4 m thick, erosive base, lenticular shape. Three to five stages fill the channel	Development and evolution of channels crossing the floodplain, probably as a result of avulsion	Eslida and Alcotas Formations (Collinson and Thompson, 1982; Allen, 1984; Ashley, 1990)
Ephemeral isolated channels (I.br)	St, Sp, Sh, Sl, Se	Width <20 m, 0.2–0.8 m thick. Very gentle erosive base and almost tabular shape. A single stage fills the channel	Development and evolution of channels produced during short periods of flow following local and intense rainfall	Eslida and Alcotas Formations (Picard and High, 1973; Dreyer, 1993)
Ribbon sandstone (In)	Se, St, Sh, Sl	W/D<15, with 'wings'. Storeys <4.5 m thick. Isolated channels bounded by floodplain deposits	Isolated anastomosed fluvial channels	Eslida Formation (Miall and Gibling, 1978; Long, 1978; Eberth and Miall, 1991)
Lateral-accretion macroforms (I.me)	St, Sh, Sl, Sp	Isolated examples. Fine grained facies, associated wedge shape	Isolated meandering fluvial channels	Eslida and Alcotas Formations (Puigdefábregas and Van Vliet, 1978)
Laminated sand sheets (ob)	Sh, Sl and less commonly Sp	<30 m long. Thin (<0.3) tabular lamina	Flash-floods depositing sand under upper flow regime, plane bed conditions	Eslida, Cañizar and Alcotas Formations (Rust and Nanson, 1989)
Crevasse splay (ob)	St, Sr	Sheet-like bodies <1 m thick and 10–100 m across. Laterally pass to fine deposits. Rarely crevasse channels are observed	Progradation from crevasse channel into floodplain	Alcotas and Eslida Formations (Gersib and McCabe, 1981; Brierley, 1991; Mjøs et al., 1993)

Several main body geometries were distinguished in the alluvial sediments of the units under study. These were considered as related to two main body geometries: isolated (I) or amalgamated (A) (Fig. 4). Isolated bodies have a general lenticular geometry and are interpreted as mostly short-lived structures and/or lateral-accretion macroforms, while amalgamated bodies represent multilateral, multi-storey complexes or belts of tabular geometry including different internal bedforms and channel forms. The isolated geometries referred to here include refill of braided channel (I.br), meander (I.me) and ribbon (I.ri), as well as, overbank deposit (o.b) morphologies. "Nested" (I.ri.me) geometries represent vertical stacking of very close superimposed ribbon geometries, which would also constitute an amalgamated geometry.

The stacked distribution of these body types, as observed in the units examined, represent the general alluvial architecture style of each one. Some of the units show different body types from base to top, indicating non-homogeneous processes affecting sedimentation during their development.

These body geometries are separated by bounding surfaces of different order (as described by Allen, 1983; Miall, 1988, 1991; Bridge, 1993; Miall, 1996, among others) that define their external morphology and separate them from adjacent bodies (Fig. 4). The range of these bounding surfaces also indicates the time needed for their development and the extent of their relationship with basin development. The eight bounding surfaces of Miall's classification (1991) can be easily differentiated in the units — from a single set bounding surface (ripple) deposited in seconds of 1st order, or macroform, seasonal event (3rd order) to a channel belt related to a fault pulse (6th order) or basin-fill complex of tectonic origin (8th order) that could last up to 10^7 years (Figs. 4 and 5).

Sixth order surfaces are thought to be of tectonic origin, due to individual pulses of the basin boundary faults that lead to changes in the rate of creation of accommodation and regional slope gradient over periods of about 1 My. Seventh and 8th order surfaces, however, represent major tectonic events, such as the beginning of extension in the basin with the appearance of new basin boundary-fault systems, causing major changes in basin geometry and regional slope (changes in fluvial style, palaeocurrent patterns, etc.) within a period of 3 to 5 My.

Accordingly, the major order bounding surfaces are mostly related to the objectives of our work, including contacts between units. Surfaces lower than 5th order are only briefly examined since they represent changes caused by autocyclic processes with estimated periods of 10^3–10^4 years for 3rd to 5th order surfaces. In contrast, 6th to 8th order surfaces represent several principal allogenic factors controlling fluvial architecture over periods of different magnitude.

Conformable contacts occur between the Boniches and Alcotas Fms, and the Eslida and Marines Fms (Fig. 2). These two contacts are similar, although in the latter case the upper unit is not purely fluvial but partly of estuarine origin. Discordances or angular unconformities are found at the base and top of the Cañizar Fm. The base of the Boniches Fm represents the basal unconformity of the Permian–Triassic alluvial sediments on the Lower Palaeozoic basement, thus represented by an 8th bounding surface, reflecting the beginning of the infilling of the sedimentary basin for most of the Iberian Ranges (Fig. 5).

The base of the Cañizar Fm is a 7th order type surface and as such represents the main reorganization of the sedimentary basin after a tectonic pulse of extensional character. Another 7th order type of change in the origin of the tectonic regime is represented at the top of the Cañizar Fm, from Chelva to some tens kilometres north of Cañete. This surface marks the absence of the Eslida and Marines Fms and is represented by iron-rich crusts, palaeosoils and bleaching of the uppermost 15 m of the fluviatile Cañizar Fm sandstones. A 7th order surface is also represented by the base of the Cañizar Fm, marked by a drastic change in fluvial environment deposition. The Cañizar Fm shows six sequences bounded by 6th order surfaces (photograph in Fig. 5) that represent sequences related to periodic basin-margin fault movements (López-Gómez and Arche, 1993b).

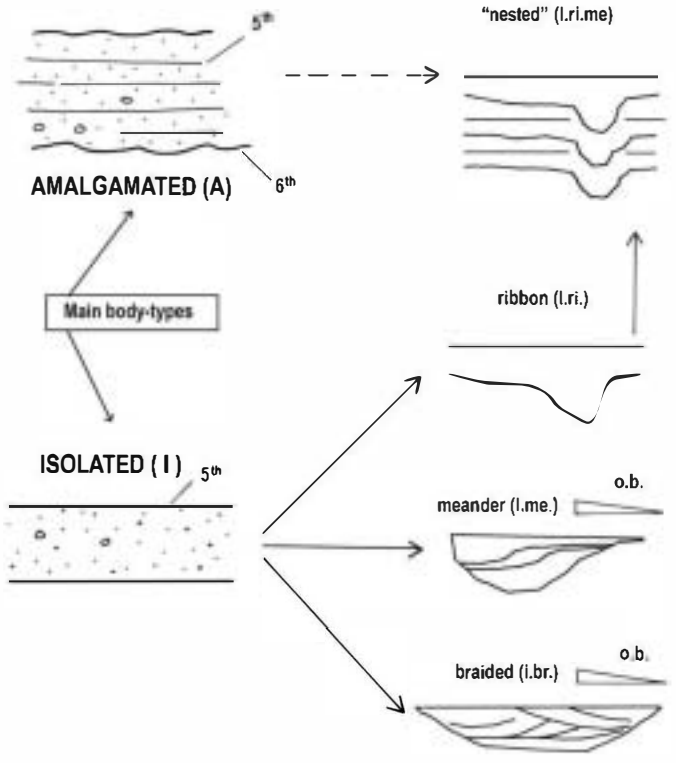

Fig. 4. Main alluvial body types differentiated in the studied formations. 5th and 6th indicate surface order following Miall's classification (1985).

5. Subsidence controlling fluvial architecture

A wide variety of sedimentary process scales control fluvial architecture. Thus, channel morphology changes downstream in response to changes in valley slope, sediment load, bank materials, or the climate or tectonic regime (Burnett and Schumm, 1983). However, on a basin time scale (10^6–10^8 yrs), tectonic control plays an essential role in macroarchitecture in terms of the fluvial style and rate of subsidence (Leeder, 1993). As, our study focuses on this time scale, we therefore considered subsidence as a basic control factor for the alluvial architecture (macroarchitecture) of each study unit. The other main control is the general base-level change or bay-line changes. In our case study, eustatic or general base-level changes were irrelevant to the fluvial architecture of the Permian–early Triassic deposits of the Iberian Basin because, for most of this time-interval, this basin was an interior basin (Arche and López-Gómez, 1999a).

Different works have modelled the interrelationship between subsidence and large-scale fluvial architecture running through the avulsion rate constant (Allen, 1978; Bridge and Leeder, 1979; Bridge and Mackey, 1993, among others). Flume experiments, however, considered that the avulsion rate, which also depends on sedimentation frequency, is not constant, and is therefore also responsible for alluvial architecture (Bryant et al., 1996; Heller and Paola, 1996). On the other hand, field studies performed on Carboniferous fluvial deposits in Scotland (Read and Dean, 1982) have also indicated that models of stacking and interconnection of sediment bodies are contrary to those predicted by Allen (1978) and Bridge and Leeder (1979).

The relationship between the avulsion rate and aggradation rate, and therefore between subsidence and avulsion, is still unclear. We only attempted to relate the presence or absence of different fluvial architectural bodies in the study units to the different crust and lithospheric mantle stretching factors (δ and β, respectively). Our aim was to increase current understanding on interrelationships among subsidence, large-scale fluvial architecture and avulsion rates.

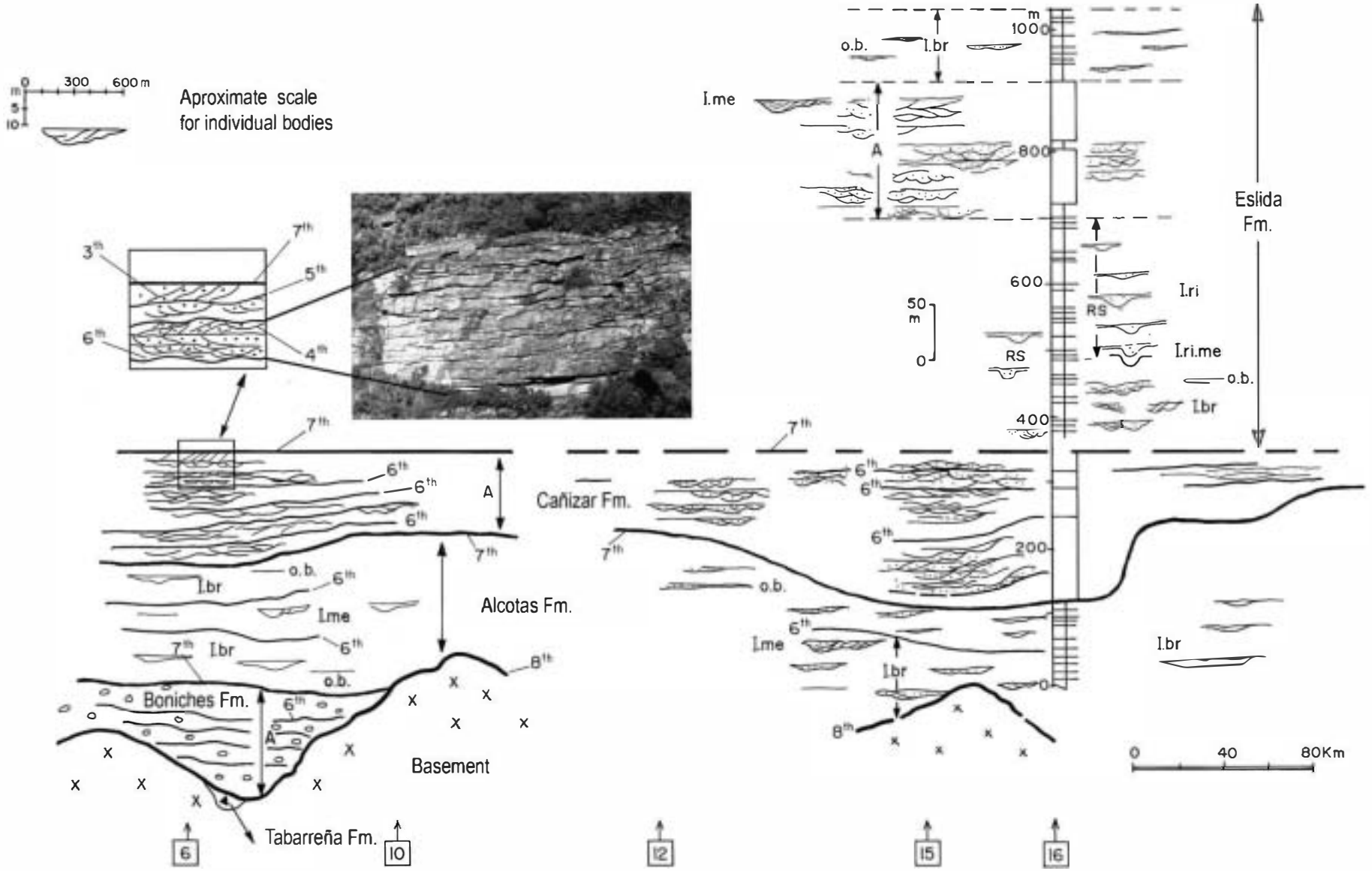

Fig. 5. Simplified scheme of the main alluvial body type observed in the studied sections. 3th to 8th indicate surface order following Miall's classification (1985). Location of the sections: 6 — Cañete, 10 — Chelva, 12 — Jérica, 15 — Gátova, and 16 — Chovar–Eslida. See also Fig. 4 for the body types and Fig. 1 for the location of the sections in the Iberian Ranges.

6. Depth-dependent subsidence analysis

6.1. Methodology

Changes in basin subsidence during the Permian and Mesozoic were analysed by the backstripping technique (Steckler and Watts, 1978; Bond and Kominz, 1984) on data obtained from complete wells and stratigraphic sections. To isolate the effect of tectonics on subsidence history, we had to correct for the effects of superimposed eustatic oscillations, palaeobathymetry changes and sediment compaction with increasing loading.

Palaeobathymetry was estimated from sedimentary facies, fossils and depositional environments as always less than 75 m for the different middle Mesozoic to Cenozoic marine intervals. Eustatic sea-level variations for the marine intervals were not introduced since estimated fluctuations are less than 100 m and would similarly affect all the wells and sections. The possible upstream effects of these variations in post-Triassic sediments are of no concern for this paper. The Permian and Early Triassic basins were far away from the Paleotethys sea and were not affected by sea-level fluctuations. Porosity–depth relations used for compaction corrections were defined according to Sclater and Christie (1980).

Since during the Cenozoic, tectonic patterns other than rifting (basin inversion in the Iberian Basin and foreland sedimentation in the Ebro Basin) and flexural and topographical effects took place (van Wees and Beekman, 2000), we omitted this period from our study.

After constructing total subsidence and air-loaded tectonic subsidence curves by backstripping and defining extensional phases in the tectonic subsidence curves, we calculated stretching factors (δ for the crust, β for the lithospheric mantle) for each synrift and postrift phase and for each section or well by forward modelling (van Wees et al., 1996). Using this model, an unlimited number of stretching phases can be introduced and the model automatically finds the best fit stretching parameters for the subsidence data, that is, $\beta = \delta$ or $\beta \neq \delta$. This means that subsidence is conditioned by mechanisms corresponding to either a single layer (i.e., the crust and lithospheric mantle show a similar rheological response) or two layers (i.e., the crust and lithospheric mantle show a different rheological response). We do not provide the calculus method in this paper, since it is well described in van Wees et al. (1998), Vargas (2002) and Vargas et al. (2009).

For the forward modelling, we assumed an initial crustal thickness of 32 km corresponding to its present-day value beneath the Iberian Massif (Banda et al., 1983), a thickness also adopted for the Iberian Ranges by Salas and Casas (1993), van Wees and Stephenson (1995) and van Wees et al. (1998), and an initial lithospheric thickness of 110 km used for the Iberian Basin by Morgan and Fernández (1992), van Wees and Stephenson (1995) and van Wees et al. (1998). The other parameters used in the model shown in Table 2 were obtained from van Wees and Stephenson (1995).

Table 2
Parameters used in the forward model (obtained from van Wees and Stephenson, 1995).

Parameter	Value
Initial crust thickness	32 km
Initial lithospheric thickness	110 km
Asthenospheric temperature	1333 °C
Thermal diffusivity	1×10^{6} m^2 s^{-1}
Surface crustal density	2800 kg m^{-3}
Surface mantle density	3400 kg m^{-3}
Water density	1030 kg m^{-3}
Thermal expansion coefficient	3.2×10^{-5} °C

6.2. Subsidence curves and phases

To obtain a wide range of subsidence data, we selected and analysed eleven sections and five boreholes. Sections are mainly located in the centre of the study area, while boreholes correspond to the western and northeastern flanks of the Permian–Triassic basin (Fig. 1), where the Cenozoic cover does not allow for direct observation.

Fig. 6 shows the tectonic subsidence curves obtained for each section or well. Most of these computations as well as the phases observed in the subsidence analysis for the whole Permian and Triassic of this basin were described in van Wees et al. (1998), Vargas (2002) and Vargas et al. (2009), so the details can be found in these bibliographic references. Our subsidence analysis indicates that the Iberian Basin experienced a number of pulsating phases of rapid tectonic subsidence followed by slower thermal subsidence phases from the Late Permian to Lower Triassic (Fig. 7). These changes in subsidence rate can, in most cases, be correlated over the entire study area.

There are two zones (Molina de Aragón and Cañete) in which extension started during the Lower Permian (Autunian phase) (290–

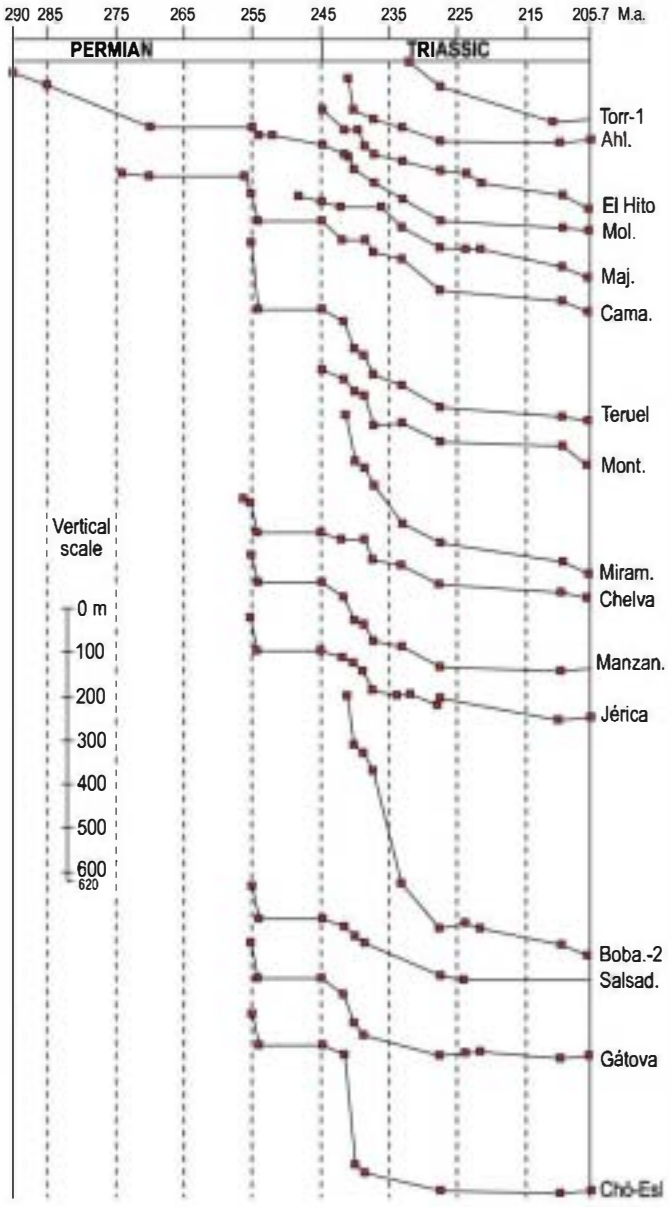

Fig. 6. Tectonic subsidence curves for the different studied sections for the Permian–Triassic interval. See Fig. 1 for the location of the sections.

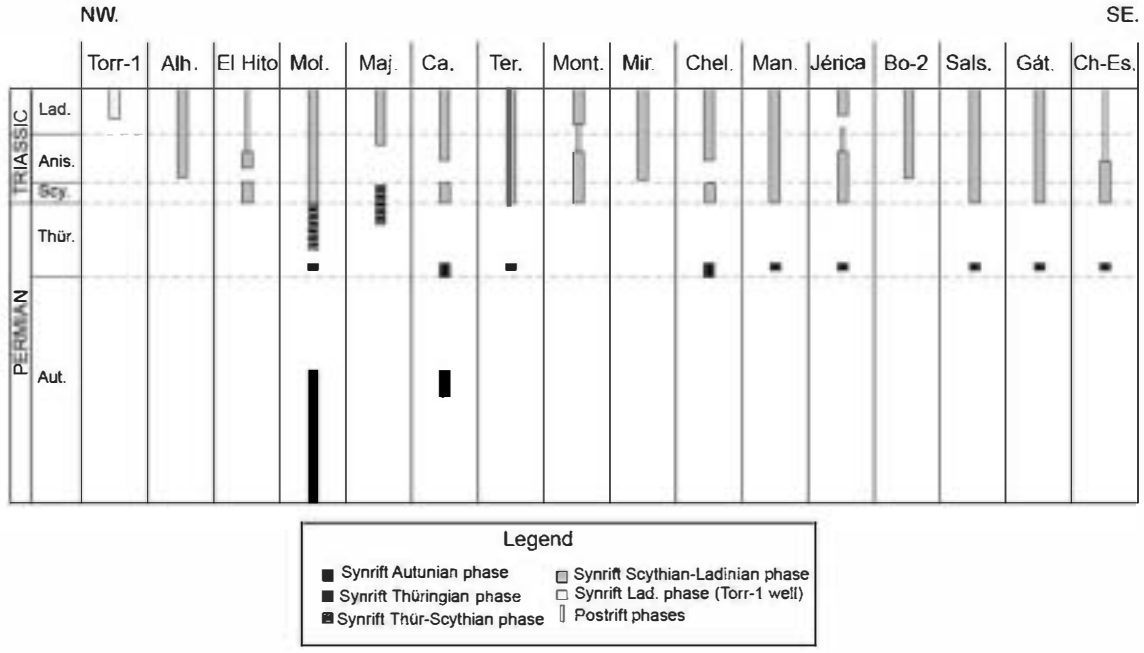

Fig. 7. Synrift and postrift identified phases in the different studied sections for the Permian–Middle Triassic interval. See Fig. 1 for the location of the sections.

270 M.a.). However, the first generalized phase for most of the study area (Thüringian phase) (255–254 M.a.) was short in time and includes most of the Late Permian sediments of the study area represented by the Boniches and Alcotas Fms. A punctual (not studied here) phase (Thüringian–Scythian) (244.8–238.5 M.a.) was differentiated for the Molina de Aragón–Majadas area. The last phase studied (Scythian–Ladinian) is related to the Cañizar and Eslida Fms. This phase was interrupted in some areas (e.g., Chelva and Cañete) or linked to a "postrift" phase (e.g., Montalbán, Chovar–Eslida) (Fig. 7).

6.3. Crust and lithospheric mantle stretching factors

As previously stated, to establish a quantitative framework for the pulsating rift changes of the lithosphere occurring during the period of time examined here, we quantified extension rates by forward modelling the tectonic subsidence analysed previously using an automated forward modelling technique (van Wees et al., 1996).

The results of this technique (Vargas et al. 2009) indicate a better fit of the stretching values calculated for most of the tectonic phases by the two-layer stretching model than the uniform one-layer stretching model, which considers a similar stretching value for the lithospheric mantle and crust. To illustrate the improved fitting of the two-layer model, we compare in Fig. 8 the application of the two models to the Cañete section. This figure shows all the Permian–Mesozoic phases (starting and ending times) although we only focus on the Autunian, Thüringian and Scythian–Ladinian phases (274–270, 256–254, and 244.8–241.8 My, respectively) that include most of the sediments examined here. The values of both stretching factors are automatically obtained for each phase by the computer program as described Vargas et al. (2009). These latter authors also demonstrated the improved fitting of the two-layer model in almost all of the fourteen sections and boreholes studied in the Permian–Middle Triassic rocks of both Iberian and Ebro Basins. It indicates that depth (crust and lithospheric mantle) dependent stretching model ($\delta \neq \beta$) fits better for the sedimentary basin filling analysis of the studied units. It is very important to differentiate one-layer and two-layer stretching processes because they lead to different basin configurations. The former will create symmetrical grabens bounded by vertical basins boundary faults, like those modelled by McKenzie (1978), but the latter will create half-graben basins bounded by listric faults flattening out at 12–15 km, as in the case of the Iberian and Ebro basins.

Fig. 9 shows β and δ stretching factor values for representative sections selected on the basis of their geographical location and complete sedimentary record for the three tectonic examined phases.

7. Fluvial architecture response

The different body geometries distinguished in the study sediments were classified as two main simplified types: isolated and amalgamated (Fig. 4). The Boniches and Cañizar Fms show amalgamated geometries, while the Alcotas and Eslida Fms show both amalgamated and isolated geometries, indicating a more complex fluvial style evolution pattern, especially for the latter formation, which also presents ribbon and nested subtypes.

The stretching factors calculated for each tectonic phase did not differ substantially. Fig. 10 contrasts β and δ data for the differentiated phases and shows how β values were almost always around 1 for all these phases, while δ values that ranged from 0.985 to 1.16 β values were always lower than δ values up to 1.002. Highest β and δ factors were shown by phases 255–254 My and 244.8–238.5 My, respectively.

To evaluate the fluvial architecture response to the different stretching factors for each tectonic phase, we established a relationship among all these data for each study unit. Fig. 11 provides this information for four selected sections in which the best outcrops are found: Cañete, Teruel, Chelva and Chovar–Eslida. Squares with no information in the figure are units not represented in the area, since only the Alcotas and Cañizar Fms occur across the whole study area. One of the main effects of tectonic subsidence in half-graben basins such as the Iberian Basin is a lateral tilting of the depositional surface as regional slope changes to adapt to differential subsidence rates (Leeder and Alexander, 1987; Alexander and Leeder, 1987; Blair and Bilodeau, 1988). Lateral tilting results in channel lateral migration, either by (a) repeated instantaneous avulsion events if the tilting (and subsidence) rate is high, or (b) slow lateral migration of the active channel belt or "combing" (Todd and Went, 1991). The first process produces isolated sand ribbons and immature channel belts embedded in floodplain fines whereas the second one tends to produce wide, multilateral, multi-storey sandstone channel belts. Examples of both types will be discussed later on.

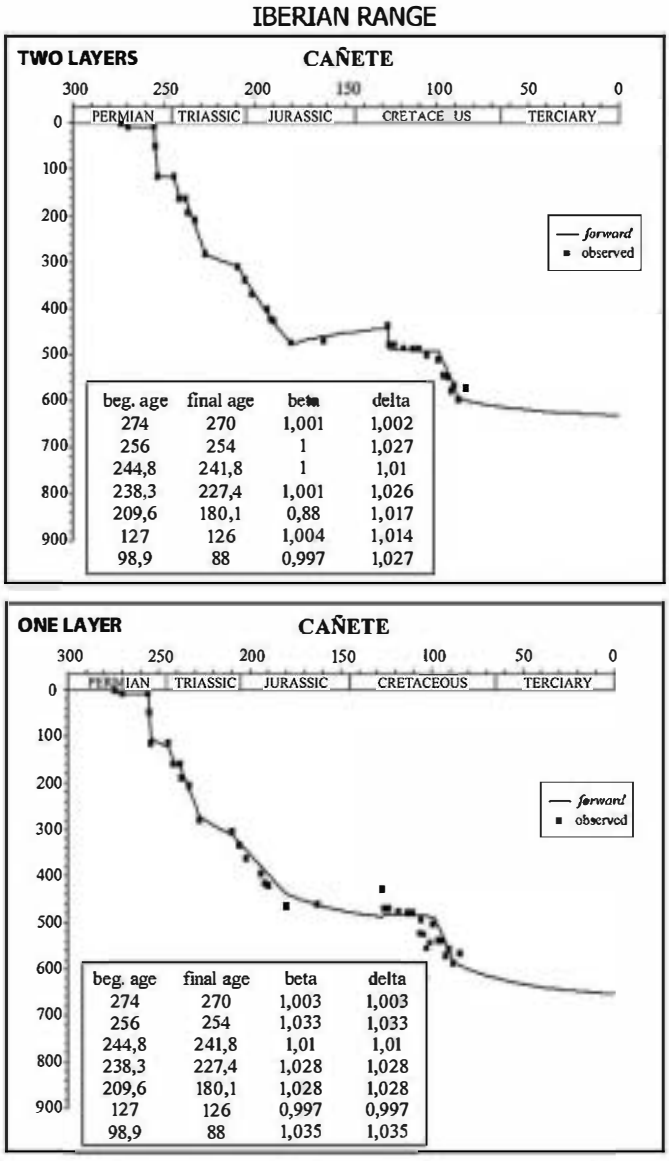

Fig. 8. Comparison of the application of both two-layer and uniform (one-layer) stretching models to the Cañete section to demonstrate the better fit of the first one.

Tectonic phase 244.8–241.8 My is the only one showing amalgamated forms as the only geometry. For this case, β and δ values are similar and very close to 1, indicating that extension was short and that the lithosphere deformed as a single layer instead of two differentiated layers corresponding to the crust and lithospheric mantle.

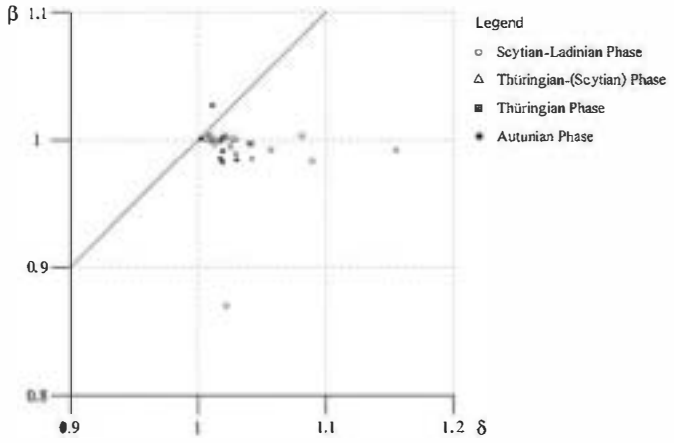

Fig. 10. Contrasted values of β and δ factors for the differentiated phases.

Sections showing the most varied architectural geometries, including ribbon and nested forms, corresponded to the highest β and δ factors (Chovar–Eslida section of the Cañizar and Eslida Fms), also reflecting tectonic phases of greater stretching and subsidence. In contrast, the same amalgamated geometry type observed in the Cañizar and Eslida Fms, both consisting of sandstones of similar characteristics and thicknesses, could have formed over short and long periods of time, i.e., less than 1 My for the Eslida Fm and more than 3 My for the Cañizar Fm.

Tectonic phases with a wider variety of fluvial geometries, such as phases 244.8–227.4 and 244.8–238.5 My, showed a greater difference in β and δ factors, indicating stages of basin development related to different crust and lithospheric mantle activity. Conversely, when the β and δ factors were close (phase 244.8–241.8 My), a reduced tendency to show different geometries was observed.

Collectively, our field and laboratory data suggest that although general subsidence in some way controls the resultant fluvial geometry of the Permian and Triassic alluvial sediments of the Iberian Ranges, there is no simple direct relationship between the two factors. The only correlation found was between crustal and lithospheric mantle activity — reflected by their stretching factors — and fluvial geometry. It would appear that, besides subsidence, we need to consider a combination of other factors such as the rate of avulsion, climate, or budget of sediments to predict the alluvial architecture of a basin.

Rates of avulsion are predicted to be high if rates of subsidence and induced lateral tilting are high. This is the case of the Eslida Fm. (Middle Triassic, Anisian) in the central-SE Iberia, especially in the lower two thirds of the formation (Arche and López-Gómez, 1999a,b), where four superimposed sedimentary cycles of coarsening-thickening type show isolated fluvial channel sandstone bodies, paleocurrent dispersion

Phases / Wells	Autunian		Thüringian		Scytian-Ladinian	
	δ	β	δ	β	δ	β
Torr-1	---	---	---	---	---	---
Mol	1.03	0.989	1.011	1.026	1.042	0.996
Alh	---	---	---	---	1.022	0.87
Ca	1.002	1.001	1.027	1	1.01/1.026	1/1.001
Ter	---	---	1.04	0.997	1.056	0.992
Chel	---	---	1.02	1.002	1.005/1.025	1.001/0.998
Ch-Esl	---	---	1.017	0.984	1.067/1.009	1.002/0.915

Fig. 9. Values of β and δ factors calculated for the differentiated phases in the selected most representative sections.

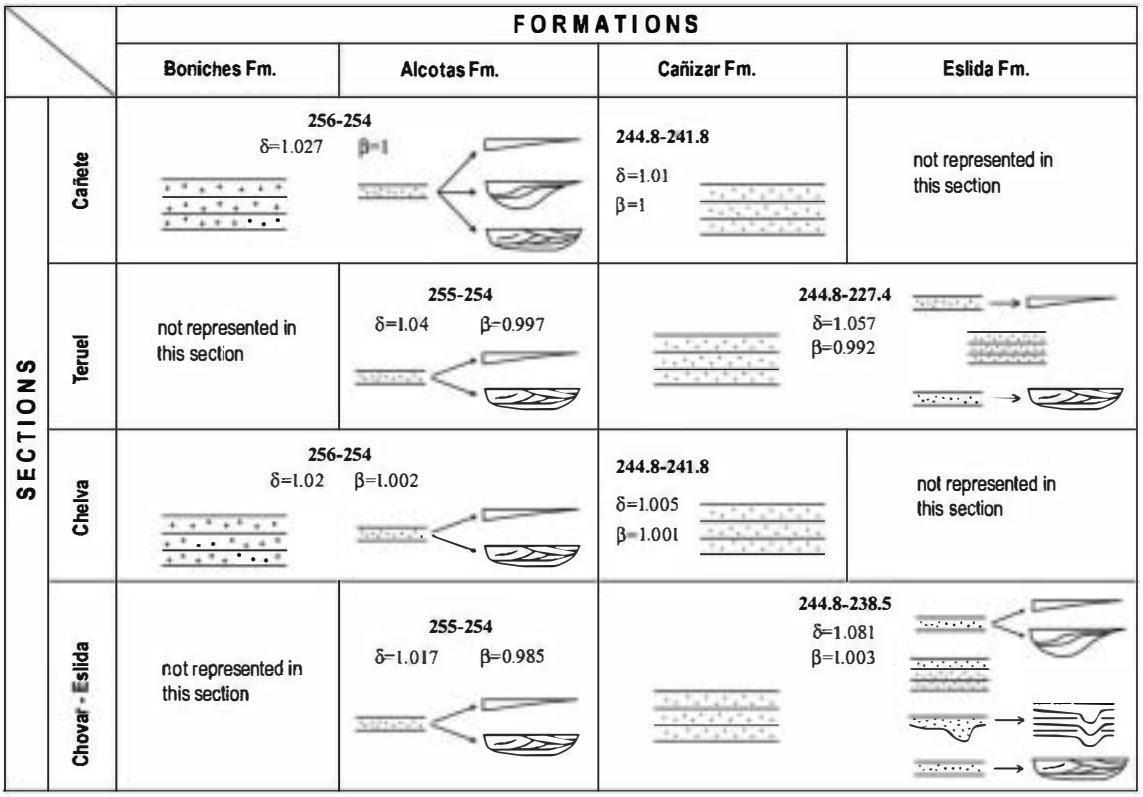

Fig. 11. Contrasted synrift phases, β and δ stretching factors values and alluvial body types for the studied units in the most representative sections. See Fig. 4 for the classification (meaning) of the body types.

ranging from 90° to 140° degrees and channel/floodplain rates lower than 10%, all consistent with high rates of subsidence and lateral tilting of the floodplain surface.

The rapid changes in basin configuration due to active subsidence in a half-graben basin in this period is well illustrated in Arche and López-Gómez (1999a,b), especially the lateral onlapping on the basement of the Eslida Formation.

A contrasting case, where low rates of subsidence and of lateral tilting lead to a "combing" process of sedimentation resulting in amalgamated multilateral, multi-storey fluvial sandstone fluvial sandstone bodies are found in the Cañizar Sandstone Formation (López-Gómez and Arche, 1993a) and the upper third of the Eslida Formation, also displaying a narrowed paleocurrent dispersion (60°–90°). The internal major bounding erosional surfaces are interpreted as rapid geomorphic response to tectonic subsidence pulses in the basin boundary fault.

8. Discussion

The vertical alluvial record of the Permian–Early Triassic period in the SE Iberian Basin and the geometry and internal structure of the alluvial sandstone bodies is the result of the complex interaction between two main factors: subsidence (a pure tectonic process) and changes in the regional and/or general base level (a mixed climatic–tectonic process) (Schumm, 1977; Bull, 2007). Avulsion rate is another independent factor controlling the character of the alluvial vertical succession for Heller and Paola (1996).

Sea-level changes (general sea-level changes) are irrelevant in our case because the alluvial sediments studied here were deposited in continental interior basins (Permian), hundreds of kilometres away from the Paleothethys sea (Triassic) (Arche and López-Gómez, 1996, 1999a,b).

Subsidence is the main control of the overall vertical successions and sandstone body geometries in the studied sediments. Amalgamated, complex tabular geometries are formed only with values of β and δ very close to 1 (very slow subsidence) both in the Cañizar Fm. for a period of about 3 M y and the top of the Eslida Fm., for a much shorter time span (Fig. 11). In the former case, the synrift period was one of very low extension rate and subsequent small creation of accommodation, whereas the latter is situated at the end of the synrift period, when extension rates seemingly decreased significantly. In both cases, factors β and δ have values lightly >1.

An important aspect of our study is that, in the interpreted two-layer configuration of the extensional lithospheric mechanism, the variations of the β factor, that is, of the behaviour of the lower part of the lithospheric plate, do not have any influence on the vertical stacking and the internal geometry of the alluvial sediments in our case, because any configuration can be found with β values >1 or <1. For example, ribbon and isolated geometries in the Alcotas and Eslida Fms. or amalgamated geometries in the Cañizar Fm. (Fig. 11). Instead, this two-layer stretching process is responsible of the large half-graben configuration of the Permian–Triassic Iberian Basin.

As a consequence, we can affirm that only the δ factor is relevant in the analysis of the tectonic control of the vertical successions and internal geometries of the alluvial sediments studied in this paper and, may be, in other similar sediments; that is, that only the mechanical behaviour of the upper lithospheric layer has influence on the alluvial succession geometries. The importance of tectonic subsidence in fluvial styles on semi-arid enclosed basins is well illustrated, for example, by Lopez et al. (2008) in the Lower Permian Lodève Basin, SE France. Lateral tilting caused by subsidence is the direct factor controlling fluvial architecture in these basins.

Values of the δ> 1.017 lead to isolated sandstone body geometries with different types of internal refill: braided (I.br.), meandering (I.me) and ribbon (I.ri.) in the Alcotas and Eslida Fms (Figs. 5 and 11) probably due mainly to multiple changes of regional slope and subsequent increased instability and avulsion events. The importance of regional slope changes in avulsion processes is pointed out by Mackey and Bridge

(1995) and Slingerhand and Smith (1998), but is considered as secondary factor by Heller and Paola (1996).

Here it is necessary to consider the combined importance of climatic factor in avulsion processes leading to the creation of multiple, isolated sandstone bodies embedded in floodplain-lacustrine siltstones. Heller and Paola (1996) stress that avulsion frequency is more strongly controlled by variations in sedimentation rate that by the total amount of sediments entering the basin. The climate was strongly seasonal in the Iberian Basin in this period (Arche and López-Gómez, 1999a,b), favouring sudden rain outburst that caused crevasse splays and the initiation of avulsion processes, already propitiated by regional slope changes of tectonic origin.

The isolated sandstone body geometries compare well with the configurations of ribbon bodies described by Möring et al. (2000) in the late Oligocene Guadalupe–Matarreña system of the Ebro basin, Spain, in which there are also examples of the "nested" geometries in some ribbons. These latter geometries result from repeated re-occupation of the abandoned channel tracts by new, active stream sections emplaced in the floodplain after an avulsion episode, as illustrated by present-day examples of western Brazil (Assine, 2005) and NE India (Jain and Sinha, 2003, 2004).

The overall vertical record of the alluvial sediments of the Permian–Early Triassic period of the Iberian Basin is controlled by changes in the δ factor of the crustal basement during synrift periods, that induce lateral tilting of the floodplain surface at different rates, whereas the internal geometry of the infilling of the isolated sandstone bodies can be the results of combined tectonic and climatic factors.

9. Conclusions

Our study is centred on the alluvial Permian and Triassic sediments of the SE Iberian Ranges and represents a first attempt at evaluating relationships between fluvial architecture and subsidence through detailed sedimentological field data and backstripping automated forward modelling. Using this combined approach, we were able to relate fluvial geometries to crust and lithospheric mantle stretching factors (δ and β respectively). The main conclusions to be drawn from our findings are:

- Depending on the tectonic phase, subsidence differently affected the two lower and upper layers of the lithosphere, rather than similarly affecting homogeneously the entire lithosphere. This two-layer configuration explains the half-graben nature of the Iberian Basin in the Permian–Triassic times.
- A complex interaction between subsidence and changes in regional base level (including its control by avulsion and climatic factors) is the cause of the vertical alluvial record and the geometry and internal structure of the conglomerate and sandstone bodies of the Permian–Early Triassic sediments in the SE Iberian Basin.
- Regional base-level changes in the Permian–Early Triassic Iberian Basin were created by tectonic movements that induced lateral tilting of the floodplain surface while sea-level changes were irrelevant to the nature of the alluvial record.
- Amalgamated, complex tabular geometries in the alluvial sediments are formed only with β and δ very close to 1 (but > 1) values (very slow subsidence), in the Cañizar and Eslida Fms. showing similar characteristics and thicknesses. Although extension rates were different in each case, this suggests that extension was limited, short-lived and that the lithosphere moved as a single layer.
- This same amalgamated geometry types observed in the Cañizar and Eslida Fms were deposited over both long (about 3 My) and short (less than 1 My) periods of time, respectively. This might imply that some geometries are not always time-dependent.
- Variations in the lower part of the lithospheric plate (β factor), in our case, do not have any relevance on the vertical stacking and the internal geometry of the alluvial sediments but only on the general configuration of the sedimentary basin. Any configuration (ribbon, isolated, amalgamated geometries) can be found with β values > 1 or < 1. Only the extension rates of the upper crust (δ factor) are relevant on the vertical stacking and the internal geometry of the alluvial sediments.
- Values of δ factor > 1.017, in our study, led to isolated sandstone bodies geometries, including different types of internal refill (braided, meandering, and ribbon). Multiple changes of regional slope led to an increase in the instability of fluvial channels and avulsion events. A climate control, superimposed to the tectonic component, could exert some control on the type of internal refill.
- Sections showing the most varied architectural geometries, including ribbon and nested forms, are related to higher β and δ factors indicating tectonic phases of greater stretching and subsidence values.
- Tectonic phases of wider ranging fluvial geometries were associated with more largely differing β and δ factors which also suggests stages of basin development in which crust and upper mantle activities differed. Conversely, closer β and δ factors were related to a tendency towards amalgamation and reduced variation in fluvial geometries.

Acknowledgements

Tectonic subsidence and forward modelling were conducted at the Faculteit der Aardwetenschappen, Vrije Universiteit, Amsterdam in collaboration with Drs. S.A.P.L. Cloetingh, J.D. van Wees and J. Gaspar-Escribano. We thank these colleagues for their help and kind hospitality during the stay of Dr. Vargas at the Vrije Universiteit. This research was supported by projects CGL2005-01520BTE and CGL2008-00093BTE. We would like to thank the commentaries of Gert Jan Weltje and an anonymous reviewer that improved an earlier version of this manuscript. We also thank Ana Burton for reviewing the English.

References

Alexander, J., 1992. Nature and origin of a laterally extensive alluvial sandstone bodie in the Middle Scalby Formation. J. Geol. Soc. Lond. 149, 431–441.

Alexander, J., Leeder, M.R., 1987. Active tectonic control on alluvial architecture. In: Ethridge, F.G., Flores, R.M. (Eds.), Spec. Pub. Soc. Econ. Paleon. Miner., vol. 39, pp. 243–252.

Allen, J.R.L., 1978. Studies in fluvial sedimentation: an exploratory quantitative model for the architecture of avulsion-controlled alluvial studies. Sediment. Geol. 21, 129–147.

Allen, J.R.L., 1983. Gravel overpassing on humpback bars supplied with mixed sediment: examples from the Lower Old Red Sandstone, southern Britain. Sedimentology 30, 285–294.

Allen, J.R.L., 1984. Sedimentary Structures: Their Character and Physical Basis. Development in Sedimentology 30. Elsevier, Amsterdam. 663 pp.

Allen, P.H., Allen, J.R., 1990. Basin Analysis. Principles & Applications. Blackwell Scientific Publications, Oxford. 404 pp.

Arche, A., López-Gómez, J., 1996. Origin of the Permian–Triassic Iberian Basin, central-eastern Spain. Tectonophysics 266, 443–464.

Arche, A., López-Gómez, J., 1999a. Tectonic and geomorphic control on the fluvial styles of the Eslida Formation, Middle Triassic, Eastern Spain. Tectonophysics 315, 187–207.

Arche, A., López-Gómez, J., 1999b. Subsidence rates and fluvial architecture of rift-related Permian and Triassic alluvial sediments of the southeast Iberian Range, eastern Spain. Spec. Publ. Int. Assoc. Sedimentol. 28, 183–304.

Ashley, G.M., 1990. Classification of large-scale subaqueous bedforms: a new look at an old problem. J. Sediment. Petrol. 60, 160–172.

Ashworth, P.J., Best, J.L., Jones, M., 2004. Relationship between sediment supply and avulsion frequency in braided rivers. Geology 32, 21–24.

Assine, M.L., 2005. River avulsions on the Taquari megafan, Pantanal wetland, Brazil. Geomorphology 70, 357–371.

Banda, E., Udías, A., Mueller, S., Mezcua, J., Boloix, M., Gallart, J., Aparicio, A., 1983. Crustal structure beneath Spain from deep seismic sounding experiments. Phys. Earth Planet. Inter. 31, 277–280.

Blair, T.C., Bilodeau, W.L., 1988. Developments of tectonic cyclotherms in rift, pull-apart and foreland basins: tectonic response to episodic tectonism. Geology 16, 7–16.

Bluck, B.J., 1976. Sedimentation in some Scottish rivers of low sinuosity. Trans. R. Soc. Edimb. Earth Sci. 69, 425–456.

Bond, G., Kominz, M.A., 1984. Construction of tectonic subsidence curves for the Early Paleozoic miogeocline, southern Canadian Rocky Mountains: implications for subsidence mechanisms, age of break up, and crustal thinning. Geol. Soc. Amer. Bull. 95, 155–173.

Boulouard, Ch., Viallard, P., 1982. Réduction ou lacune du Tias Inférieur sur la bordure meditérranne de la Chaine Ibérique: Arguments palynologiques. C. R. Acad. Sci. Paris 295, 803–808.

Bridge, J.S., 1993. The Interaction Between Channel Geometry, Water Flow, Sediment Transport and Deposition in Braided Rivers. In: Best, J.L, Bristow, C.S. (Eds.), Braided Rivers: Geol. Soc., London, Spec. Publ., vol. 75, pp. 13–71.

Bridge, J.S., Ieeder, M.R., 1979. A simulation model of alluvialstratigraphy. Sedimentology 26, 617–644.

Bridge, J.S., Mackey, S.D., 1993. A Revised Alluvial Stratigraphy Model. In: Marzo, M., Puigdefábregas, C. (Eds.), Alluvial Sedimentation: Inter. Assoc. Sediment., Spec. Publ., vol. 17, pp. 319–336.

Brierley, G.J., 1991. Floodplain sedimentology of the Squamish river, British Columbia: relevance of element analysis. Sedimentology 38, 735–750.

Bryant, M., Falk, P., Paola, Ch., 1996. Experimental study of avulsion frequency and rate of deposition. Geology 23, 365–368.

Bull, W.B., 2007. Tectonic Geomorphology of the Mountains. Blackwell, Oxford. 316 pp.

Burnett, A.W., Schumm, S.A., 1983. Alluvial river response to neotectonic deformation in Louisiana and Mississippi. Science 222, 49–50.

Cant, D.J., Walker, R.G., 1978. Fluvial processes and facies sequences in the sandy braided South Saskatchewan River, Canada. Sedimentology 25, 625–648.

Collinson, J.D., Thompson, D.B., 1982. Sedimentary Structures2nd. Unwin & Hyman, London. 207 pp.

Cotter, E., Graham, J.R., 1991. Coastal plain sedimentation in the Late Devonian of southern Ireland: hummocky cross-stratification in fluvial deposits. Sediment. Geol. 72, 210–224.

Crowley, K.D., 1983. Large-scale bed configurations (macroforms), Platte River Basin, Colorado and Nebraska: primary structures and formative processes. Geol. Soc. Amer. Bull. 94, 117–133.

Doubinger, J., López-Gómez, J., Arche, A., 1990. Pollen and spores from the Permian and Triassic sediments of the Iberian Ranges, Cueva de Hierro (Cuenca) to Chelva-Manzanera (Valencia) region, Spain. Rev. Paleobot. Palynol. 6, 25–45.

Dreyer, T., 1993. Quantified Fluvial Architecture in Ephemeral Stream Deposits of the Esplugafedra Formation (Paleogene), Tremp-Graus Basin, Northern Spain. In: Marzo, M., Puigdefábregas, C. (Eds.), Alluvial Sedimentation: Inter. Assoc. Sediment., Spec. Publ., vol. 17, pp. 337–362.

Eberth, D.A., Miall, A.D., 1991. Stratigraphy, sedimentology and evolution of a vertebrate bearing, braided to anastomosed fluvial system, Cutler Formation (Permian–Pennsylvanian), north-central New Mexico. Sediment Geol. 72, 225–252.

Fielding, Ch., 1993. A review of recent research in fluvial Sedimentology. Sediment. Geol. 85, 3–14.

Friend, P., 1983. Towards the Field Classification of Alluvial Architecture or Sequence. In: Collinson, J.D., Iewin, J.L. (Eds.), Modern and Ancient Fluvial Systems: Spec. Publ. Int. Assoc. Sedimentol., vol. 6, pp. 345–354.

Gersib, G.A., McCabe, P.J., 1981. Continental Coal-bearing Sediments of the Port Hood Formation (Carboniferous), Cape Linzee, Nova Scotia, Canada. In: Ethridge, F.G., Flores, R. (Eds.), Recent and Ancient Nonmarine Depositional Environments: Model for Exploration: Spec. Publ. Soc. Econ. Paleont. Miner., vol. 31, pp. 95–108.

Gradstein, F.M., Agterberg, F.P., Ogg, J.G., Hardenbol, J., Van Veen, P., Thierry, Huang, J., 1995. Geochronology, time scales and global stratigraphic correlation. SEPM Spec. Publ. 54, 95–126.

Guimerá, J., Álvaro, M., 1990. Structure et evolution de la compresión alpine dans la Chaine Iberiqué et de la Chaine Cotiere Catalane (Espagne). Bull. Soc. Geol. France 6, 339–348.

Haszeldine, 1983. Descending Tabular Cross-bed Sets and Bounding Surfaces From a Fluvial Channel in the Upper Carboniferous Coalfield of Northeast England. In: Collinson, J.D., Lewin, J.L. (Eds.), Modern and Ancient Fluvial Systems: Spec. Publ. Int. Assoc. Sedimentol., vol. 6, pp. 449–456.

Heller, P., Paola, C., 1996. Downstream changes in alluvial architecture: and exploration of controls on channel-stacking patterns. J. Sediment. Res. 2, 297–306.

Hirst, J.P.P., 1991. Variations in Alluvial Architecture Across the Oligo-Miocene Huesca Fluvial System, Ebro Basin, Spain. In: Miall, A.D., Tyler, N. (Eds.), The Three-Dimensional Facies Architecture of Terrigenous Clastic Sediments, and its Implications for Hydrocarbon Discovery and Recovery: Concepts in Sedimentology and Sedimentology 3. Soc. Econ. Paleont. Miner., pp. 111–121.

Horne, J.C., Fern, J.C., 1976. Carboniferous Depositional Environments in the Pocahontas Basin, Eastern Kentuky and Southern West Virginia. Guidebook Department of Geology. University of South Carolina, Columbia. 62 pp.

Huismans, R.S., Podladchikov, Y.Y., Cloetingh, S., 2001. Transition from passive to active rifting: relative importance of asthenospheric doming and passive extension of the lithosphere. J. Geophys. Res. 106, 11271–11291.

Jain, V., Sinha, R., 2003. Hyperavulsive, anabranching Bajhmati river system, north Bihar plains, Eastern India. Z. Geomorphologie N.F. 47, 101–116.

Jain, V., Sinha, R., 2004. Fluvial dynamics of an anabranching river system in Himalayan foreland basi, Baghnati river, north Bihan Plains, India. Geomorphology 60, 147–170.

Ieeder, M.R., 1993. Tectonic Controls Upon Drainage Basin Development, River Channel Migration and Alluvial Architecture: Implications for Hydrocarbon Reservoir Development and Characterization. In: North, C.P., Prosser, D.J. (Eds.), Characterization of Fluvial and Aeolian Reservoirs: Geol. Soc. Spec. Pub., vol. 73, pp. 7–22.

Ieeder, M., Alexander, J., 1987. The origin and tectonic significance of asymmetrical meanderbelts. Sedimentology 34, 217–226.

Iong, D.G.F., 1978. Proterozoic Stream Deposits: Some Problems of Recognition and Interpretation of Ancient Sandy Fluvial Systems. In: Miall, A.D. (Ed.), Fluvial Sedimentology: Mem. Can. Soc. Petrol. Geol., vol. 5, pp. 313–342.

Lopez, M.L., Gand, G., Garric, J., Kärner, F., Schneider, J., 2008. The playa environments of the Lodéve Permian basin (Languedoc, France). J. Iber. Geol. 34 (1), 29–56.

López-Gómez, J., Arche, A., 1993a. Sequence stratigraphic analysis and paleogeographic interpretation of the Buntsandstein and Muschelkalk facies (Permo-Triassic) in the SE Iberian Range, E. Spain. Palaeogeogr. Palaeoclimatol. Palaeoecol. 103, 179–201.

López-Gómez, J., Arche, A., 1993b. Architecture of the Cañizar fluvial Sheet Sandstones. In: Marzo, M., Puigdefábregas, C. (Eds.), Alluvial Sedimentation: Spec. Publ. Int. Assoc. Sedimentol., vol. 17, pp. 317–381.

López-Gómez, J., Arche, A., 1994. La Formación Brechas de Tabarreña (Pérmico Inferior): Depósitos de flujos con densidad variable al SE de la Cordillera Ibérica, España. Bol. R. Soc. Esp. Hist. Nat. 89, 131–144.

López-Gómez, J., Arche, A., 1997. The Upper Permian Boniches Conglomerates Formation: evolution from alluvial fan to fluvial system environments and accompanying tectonic and climatic controls in the southeast Iberian Ranges, Central Spain. Sediment. Geol. 114, 267–294.

López-Gómez, J., Arche, A., Pérez-López, A., 2002. Permian and Triassic. In: Gibbons, W., Moreno, T. (Eds.), The Geology of Spain. Geological Society, London, pp. 185–212.

Mackey, S.D., Bridge, J.S., 1995. Three-dimensional model of alluvial stratigraphy: theory and applications. J. Sediment. Research 65, 7–31.

Marzo, M., Anadón, P., 1987. Evolución y características sedimentológicas de las facies fluviales basales del Buntsandstein de Olesa de Montserrat (Provincia de Barcelona). Cuad. Geol. Iber. 4, 211–222.

McKenzie, D., 1978. Some remarks on the development of sedimentary basins. Earth Planet. Sci. Iett. 40, 25–31.

Miall, A.D., 1985. Architectural-element analysis: a new method of facies analysis applied to fluvial deposits. Earth Sci. Rev. 22, 261–308.

Miall, A.D., 1988. Reservoir heterogeneities in fluvial sandstones: lesson from outcrop studies. Bull. Am. Assoc. Petrol. Geol. 72, 682–697.

Miall, A.D., 1991. Sedimentology of Sequence Boundary Within the Nonmarine Torrivio Member, Gallup Sandstone (Cretaceous), San Juan Basin, New Mexico. In: Miall, A.D., Tyler, N. (Eds.). The Three Dimensional Facies Architecture of Terrigenous Clastic Sediments and its Implications for Hydrocarbon Discovery and Recovery. Concepts in Sedimentology and Palaeontology. Soc. Econ. Palaeontol. Miner. 3, 224–232.

Miall, A.D., 1996. The Geology of Fluvial Deposits. Sedimentary Facies, Basin Analysis and Petroleum Geology. Springer Verlag, New York. 582 pp.

Miall, A.D., Gibling, M.R., 1978. The Siluro-Devonian clastic wedge of Somerset Island, Artic Canada, and some regional paleogeographic implications. Sediment. Geol. 21, 85–127.

Middleton, G.V., Trujillo, A., 1984. Sedimentology and Depositional Setting of the Upper Proterozoic Scanlan Conglomerate, Central Arizona. In: Kostner, E.H., Steel, R. (Eds.), Sedimentology of Gravel and Conglomerates: Mem. Can. Soc. Petrol. Geol., vol. 10, pp. 189–201.

Mjøs, R., Walderhaug, O., Prestholm, E., 1993. Crevasse Splay Sandstone Geometries in the Middle Jurassic Ravenscar Group of Yorkshire, UK. In: Marzo, M., Puigdefábregas, C. (Eds.), Alluvial Sedimentation: Int. Assoc. Sedimentol. Spec. Publ., vol. 17, pp. 167–184.

Morgan, P., Fernández, M., 1992. Neogene vertical movements and constrains on extensión in the Catalan Coastal Ranges, Iberian Peninsula, and the Valencia through (western Mediterranean). Tectonophysics 203, 185–201.

Möring, D., Heller, P.L., Paola, C., Lyons, W.L., 2000. Interpreting avulsion process from ancient alluvial sequences: Guadalope–Matarraña system (Northern Spain) and Wasatch Formation (Western Colorado). G.S.A. Bull. 112, 1787–1803.

Nanson, W., Croke, J.C., 1992. A genetic classification of floodplain. Geomorphology 4, 459–486.

Nemec, W., Postma, G., 1993. Quaternary Alluvial Fans in Southwestern Creta: Sedimentation, Processes and Geomorphic Evolution. In: Marzo, M., Puigdefábregas, C. (Eds.), Alluvial Sedimentation: Int. Assoc. Sedimentol. Spec. Publ., vol. 17, pp. 235–276.

Olsen, H., 1988. The architecture of a sandy braided-meandering river system: an example from the Lower Triassic Solling Formation (M. Buntsandstein) in W-Germany. Geol. Rundsch. 77, 797–814.

Ore, H.T., 1964. Some criteria for recognition of braided stream deposits. Wyo. Contrib. Geol. 3, 1–14.

Pérez-Arlucea, M., Sopeña, A., 1985. Estudio estratigráfico y sedimentológico de los materiales pérmicos y triásicos en el noroeste de la Sierra de Albarracín (Provincia de Guadalajara). Estud. Geol. 39, 329–343.

Picard, M.D., High, L.R., 1973. Sedimentary Structures of Ephemeral Streams. Elsevier, Amsterdam. 325 pp.

Puigdefábregas, C., Van Vliet, A., 1978. Meandering Stream Deposits from the Tertiary of the Southern Pyrenees. In: Miall, A.D. (Ed.), Fluvial Sedimentology: Mem. Ca. Soc. Petrol. Geol., vol. 5, pp. 469–485.

Røe, S.-L., Hermansen, M., 1993. Processes and Products of Large, Iate Precambrian Sandy Rivers in Northern Norway. In: Marzo, M., Puigdefábregas, C. (Eds.), Alluvial Sedimentation: Int. Ass. Sedimentol. Spec. Publ., vol. 17, pp. 151–166.

Ramos, A., Sopeña, A., 1983. Gravel Bars in Low-sinuosity Streams (Permian and Triassic, Central Spain). In: Collinson, J.D., Lewin, J. (Eds.), Modern and Ancient Fluvial Systems: Spec. Publ. Int. Assoc. Sedimentol., vol. 6, pp. 301–312.

Read, W.A., Dean, J.M., 1982. Quantitative relationships between numbers of fluvial cycles, bulk lithological composition and net subsidence in Scottish Namurian Basin. Sedimentology 29, 181–200.

Royden, L., Keen, C.E., 1980. Rifting process and thermal evolution of the continental marginof eastern Canada determined from subsidence curves. Earth Planet. Sci. Iett. 51, 343–361.

Rust, B.R., Legun, A.S., 1983. Modern Anastomosing-fluvial Deposits in Arid Central Australia, and a Carboniferous Analogue in New Brunswick, Canada. In: Collinson, J.D., Iewin, J. (Eds.), Modern and Ancient Fluvial Systems: Spec. Publ. Int. Assoc. Sedimentol., vol. 6, pp. 385–392.

Rust, R.B., Nanson, G.C., 1989. Bedload transport of mud as pedogenic aggregates in modern and ancient rivers. Sedimentology 36, 291–306.
Salas, R., Casas, A., 1993. Mesozoic extensional tectonics, stratigraphy and crustal evolution during the Alpine cycle of the eastern Iberian Basin. Tectonophysics 228, 33–56.
Salveson, J.O., 1976. Variations in the Oil and Gas Geology of Rift Basins. Egyptian General Petrol Corp., 5th Explor. Sem., Cairo, Egypt, pp. 25–27.
Salveson, J.O., 1978. Variations in the geology of rift basins — a tectonic model. Rio Grande Rift Symposium. Abstract. Santa Fe, New Mexico, 82–86.
Sánchez-Moya, Y., Sopeña, A., Muñoz, A., Ramos, A., 1992. Consideraciones teóricas sobre el análisis de la subsidencia: aplicación a un caso real en el borde de la cuenca Triásica Ibérica. Rev. Soc. Geol. España 5 (3–4), 21–39.
Schumm, S.A., 1977. The Fluvial System. John Wiley & Sons, New York. 338 pp.
Sclater, J.G., Christie, P.A.F., 1980. Continental stretching: an explanation of the post-Mid-Cretaceous subsidence of the Central North Sea Basin. J. Geophys. Res. 85, 3711–3789.
Slingerhand, R., Smith, N.D., 1998. Necessary conditions for a meandering-river avulsion. Geology 26, 435–438.
Sopeña, A., López-Gómez, J., Arche, A., Pérez-Arlucea, M., Ramos, A., Virgili, C., Hernando, S., 1988. Permian and Triassic Rift Basins of the Iberian Peninsula. In: Manspeizer, W. (Ed.). Triassic–Jurassic Rifting. Continental Breakup and the Origin of the Atlantic Ocean and Passive Margins. Developments in Geotectonics, 22B, Elsevier, Amsterdam, 757–786.
Sopeña, A., Doubinger, J., Ramos, A., Pérez-Arlucea, M., 1995. Palynologie du Permien et du Triassique dans le centre de la Peninsule Iberique. Sci. Géol., Bull. 48, 119–157.
Steckler, M.S., 1981. Thermal and mechanical evolution of Atlantic-type margins. Unpublished Ph.D Dissertation, Columbia University, New York. 261p.
Steckler, M.S., Watts, A.B., 1978. Subsidence of the Atlantic-type continental margin of New York. Earth Planet. Sci. Lett. 41, 1–13.
Steel, R., Ryseth, A., 1990. The Triassic–Early Jurassic Succession in the Northern North Sea: Megasequence Stratigraphy and Intra-Triassic Tectonics. In: Hardmann, R.F.P., Brooks, J. (Eds.), Tectonic Events Responsible for Britain's Oil and Gas Reserves: Geol. Soc. Lond. Spec. Publ., vol. 55, pp. 139–168.
Todd, S.P., Went, D.J., 1991. Lateral migration of sand-bed rivers: the Devonian Glashabeg Formation, SW Ireland and the Cambrian Alderney Sandstone Formation, Channel Islands. Sedimentology 38, 997–1020.
Van Wees, J.D., Beekman, F., 2000. Lithosphere rheology during intraplate basin extension and inversion. Inferences from automated modelling of four basins in western Europe. Tectonophysics 320, 219–242.
Van Wees, J.D., Stephenson, R.A., 1995. Quantitative modelling of basin and rheological evolution of the Iberian Basin (Central Spain): implications for lithospheric dynamics of intraplate extension and inversion. Tectonophysics 252, 163–178.
Van Wees, J.D., Stephenson, R.A., Stovba, S.M., Shymanovsky, V.A., 1996. Tectonic variation in the Dniepr–Donets Basin from automated modelling of backstripped subsidence curves. Tectonophysics 268, 257–280.
VanWees, J.D., Arche, A., Beijdorff, C.G., López-Gómez, J., Cloetingh, S.A.P.L., 1998. Temporal and spatial variations in tectonic subsidence in the Iberian Basin (eastern Spain): inferences from automated forward modelling of high-resolution stratigraphy (Permian–Mesozoic). Tectonophysics 300, 285–310.
Vargas, H., 2002. Análisis y comparación de la subsidencia entre las cuencas Ibérica y Ebro Central durante el Pérmico y Triásico y su relación con el relleno sedimentario. Unpublished Ph.D Dissertation. Universidad Complutense, Madrid.
Vargas, H., Gaspar-Escribano, J., López-Gómez, J., Van Wees, J.D., Cloetingh, S., De la Horra, R., Arche, A., 2009. Comparison of the Iberian and Ebro basins during the Permian and Triassic, eastern Spain: a quantitative subsidence modelling approach. Tectonophysics 474, 160–183.